Brownian motion through a two-dimensional glass: Trapping, hopping, and diffusion

Li-Shi Luo[a)]
Department of Physics, Worcester Polytechnic Institute, Worcester, Massachusetts 01609

George D. J. Phillies[b)]
Department of Physics and Associated Biochemistry Faculty, Worcester Polytechnic Institute, Worcester, Massachusetts 01609

(Received 20 October 1995; accepted 1 April 1996)

Computer simulations and computational diagnostics are used to study a Monte Carlo Brownian walker moving through a glass of immobile force centers. Clear evidence for distinct trapping, hopping, and hindered-diffusive regimes is seen in the mean-square displacement and the probability distribution $P(r,t)$ for a step r during delay t. In the hopping regime distinct time scales for intratrap and intertrap motion are apparent; probe localization and time scale separation depend inversely on temperature T. In the hindered-diffusion regime, the effective diffusion coefficient D follows an Arrhenius temperature dependence. In this regime, $\langle r^2(t)\rangle$ is very nearly linear in t, even for walkers that have only diffused a small fraction of the matrix particle nearest-neighbor distance. We infer that analytic calculations using relatively low-order time expansions should give reasonable values for D of probe particles in our glass. © *1996 American Institute of Physics.* [S0021-9606(96)50526-X]

I. INTRODUCTION

The objective of this series[1] of simulations is to gain a better understanding of experiments and other simulations of molecular and mesoparticulate motion through structured media, such as fumed silica,[2] Vycor,[3] polymers,[4] pillared clays,[5] gels[6–13] and biological cells and rigid intercellular media.[14] Probe motions have been examined with a variety of scattering techniques, including fluorescence recovery after photobleaching,[14] forced Rayleigh scattering,[2] and quasielastic light scattering spectroscopy,[6] as well as direct techniques for determining mass transfer, notably gravimetric analysis.[5] Experimental studies have been supplemented by a range of simulations. Mueller–Plathe[4] set up a matrix modeling high-density polyethylene chains having local mobility; molecular dynamics was then used to model the motion of a gas molecule through the matrix. Chen *et al.*[5] examined particle motion on a lattice in which random lines were permanently set to block probe diffusion. In these studies, molecular or Brownian dynamics methods obtained sample trajectories for a random walker. Statistical averages were performed on the trajectory, primarily calculating the mean-square displacement $\langle r^2(t)\rangle$ of a probe as a function of time and determining the effective diffusion coefficient D.

We have previously[1] reported simulations of a Brownian probe particle diffusing amidst a square lattice of immobile force centers. The probe particle interacted with force center via a 6-12 potential. Probe behavior depended qualitatively on temperature and density. Probe behavior in each temperature regime was successfully interpreted in terms of the system's potential energy surface.

Our previous simulation differed from those reported earlier in that we employed a substantially wider range of computational diagnostics, including the two-point density of states $\rho^{(2)}(\mathbf{r})$, the probability density $P(r,t)$ that after a delay t a probe will have displaced through r, and the dynamic structure factor $S(\mathbf{k},t)$. We showed, at all temperatures and densities, that these functionals of particle trajectories self-consistently characterize probe behavior.

Qualitatively, we[1] were able to resolve probe behavior into three regimes, namely trapping, hopping, and hindered diffusion. In the trapping regime, $\langle r^2(t)\rangle$ at first increased with increasing t. On reaching the trap perimeter, the probe ceased to advance; $\langle r^2(t)\rangle$ ceased to increase with increasing t. Correspondingly, in the trapping regime $S(\mathbf{k},t)$ (except at very large scattering vector k) showed very little decay, while $P(r,t)$ revealed particles that spread out to some maximal r and then spread no farther. Indeed, at large t under trapping conditions $P(r,t)$ becomes stationary. We observed uniform trapping behavior; nonergodic behavior — local trapping of some probes but not others — is impossible in our lattice because of the form of the potential energy surface. Our computational diagnostics reliably distinguished trapping, hopping, and hindered diffusion.

In the hopping regime $\langle r^2(t)\rangle$ at first increased quickly; $\langle r^2(t)\rangle$ then attained a plateau and temporarily ceased to increase. With patience hopping particles were observed to escape traps. At large t, $\langle r^2(t)\rangle$ of a hopping particle increases with increasing t. The corresponding behavior was seen in $S(\mathbf{k},t)$; this function exhibits relaxations on two time scales, reflecting intratrap and intertrap motion. Furthermore, $P(r,t)$ reveals that the spread of particles to larger and larger

[a)]Present address: Scientific Computational Methods Group (XCM), MS-F645, Applied Theoretical and Computational Physics Division (X Division), Los Alamos National Laboratory, Los Alamos, New Mexico 87545. Electronic mail address: luo@t13.lanl.gov
[b)]Author to whom correspondence should be addressed. Electronic mail: phillies@wpi.wpi.edu (Internet).

r is delayed by barriers through which penetration eventually occurs. The equilibrium two-point density of states

$$\rho^{(2)}(\mathbf{r}) = \int \exp[-\beta u(\mathbf{r}')]\exp[-\beta u(\mathbf{r}'+\mathbf{r})]d\mathbf{r}' \qquad (1)$$

confirmed that the barriers visible in $P(r,t)$ arise from the system's potential energy surface.

Finally, at high temperature $P(r,t)$ has a near-Gaussian form at all times, while $S(\mathbf{k},t)$ decays nearly exponentially to zero. These behaviors reflect uniformly hindered diffusion.

It should be emphasized that distinctions between trapping, hopping, and hindered diffusive behavior are partly a matter of time scales. At large time, a hopping particle appears to perform free diffusion, albeit with a much-reduced D. If simulations had been limited to shorter times, some colder hopping particles would appear to be trapped. Our simulations find no fundamental distinction between hopping and trapped particles. With sufficient patience, apparently all ''trapped'' particles would eventually move from trap to trap and diffuse through large distances.

The objective here is to investigate what happens when the regular lattice of force centers[1] is replaced with an irregular constellation of centers. Are there still motional regimes separated by transitions, or does the irregularity of the glass mask transitions? Computational methods are treated in Section II. Quantitative results are given in Section III. Section IV gives a discussion and our conclusions.

II. COMPUTATIONAL METHODS

Our system was a two-dimensional square surface of size 22.92×22.92 (in arbitrary distance units) with periodic boundary conditions. The matrix contained a glassy array of immobile matrix particles of two species. The 100 Species 1 particles had a radius σ_1 of 1.5, while the 400 Species 2 particles had a radius σ_2 of 1.0. The particle density ρ of the system was approximately 0.9518; matrix particles were rigidly fixed in position. The glassy array was obtained by Gould *et al.*[15] by temporarily allowing the matrix particles to move and using a molecular dynamics simulation to take the glass particles through a quenching process from high to low temperature.

We studied a single probe particle diffusing in the spaces between the matrix particles. The probe interacts with each matrix particle by a 12-6 potential:

$$u(r) = \left(\frac{\sigma}{r}\right)^{12} - \left(\frac{\sigma}{r}\right)^{6}, \qquad (2)$$

where $\sigma = \frac{1}{2}(\sigma_0+\sigma_1)$ or $\frac{1}{2}(\sigma_0+\sigma_2)$ depending on the species of the matrix particle. The probe radius σ_0 is 0.1, and σ_1 and σ_2 are 1.5 and 1.0, respectively, so $\sigma = 0.8$ or 0.55. In our simulations, we choose a cutoff interaction radius $r_{\max} = 3.0\sigma_{\max}$, where $\sigma_{\max}$ is the larger of the two values of σ. The total potential energy $U(\mathbf{r})$ of the probe included interactions with matrix particles that were less than $r_{\max}$ away from the probe. Equation (2) gives $u(r)$ in dimensionless energy units; k_BT is reported in the same dimensionless units.

The probe particle dynamics was based on the Metropolis algorithm.[16] To ensure the isotropy of the random walk, we separately generated step components δx and δy along the x and y axes, rejecting steps that did not satisfy the condition

$$\delta x^2 + \delta y^2 \leqslant r_0^2, \qquad (3)$$

where $r_0 = 0.05$. The steps δx and δy were chosen from a uniformly distributed (pseudo-)random variable.

We computed potential energy surfaces, recorded particle trajectories, and generated coarse-grained trajectory plots for many particles. We also found the mean-square displacement of the probe particles against time displacement t

$$\langle r^2(t)\rangle = \langle \|\mathbf{r}(\tau+t) - \mathbf{r}(\tau)\|^2\rangle \qquad (4)$$

by averaging over N_0 probe particles and T_0 choices of the time origin τ. The effective diffusion coefficient D is defined

$$\overline{D} = \left\langle \frac{r^2(t)}{4t} \right\rangle \qquad (5)$$

by a weighted linear-least-square fit to $\langle r^2(t)\rangle$ with weighing factor $1/t$. We also computed the probe dynamic structure function

$$S(\mathbf{k},t) = \langle e^{i\mathbf{k}\cdot[\mathbf{r}_m(t+\tau)-\mathbf{r}_n(\tau)]}\rangle \equiv \frac{1}{N_0^2}\sum_{m,n=1}^{N_0}\int e^{i\mathbf{k}\cdot[\mathbf{r}_m(t+\tau)-\mathbf{r}_n(\tau)]}d\tau, \qquad (6)$$

and the distribution function $P(r,t)$ for displacements r as a function of delay time t.

In each run, a set of ten probe particles were started at a series of randomly chosen locations and then thermalized. Determinations of $\langle r^2(t)\rangle$, $P(r,t)$, and $S(\mathbf{k},t)$ were always preceded by 1×10^6 Monte Carlo steps not included in the determination, to thermalize the locations of the probe particles. We then obtained 2×10^5 samples of $r^2(t)$, $P(r,t)$, and $S(\mathbf{k},t)$ for various time delays t with 200 Monte Carlo steps between each sample. All calculations were done on a DEC Alpha workstation. The random number generator used in the simulations was ran3() of Press *et al.*.[17]

III. RESULTS

What is the form of the local potential energy surface? Local sections are seen in Figs. 1a–1c, which also gives samplings of the position of a single particle at a series of times. Contour lines show the potential energy surfaces. Circular areas are high-energy regions near matrix particles, from which probes are excluded. The probes are confined to long, narrow regions separated by constricted saddle points.

Figure 1a shows a frozen probe at $k_BT = 0.01$. Over the entire simulation, the probe remains in a single potential energy surface minimum, never straying more than 0.03 distance units from its average position. Figure 1b ($k_BT = 0.2$)

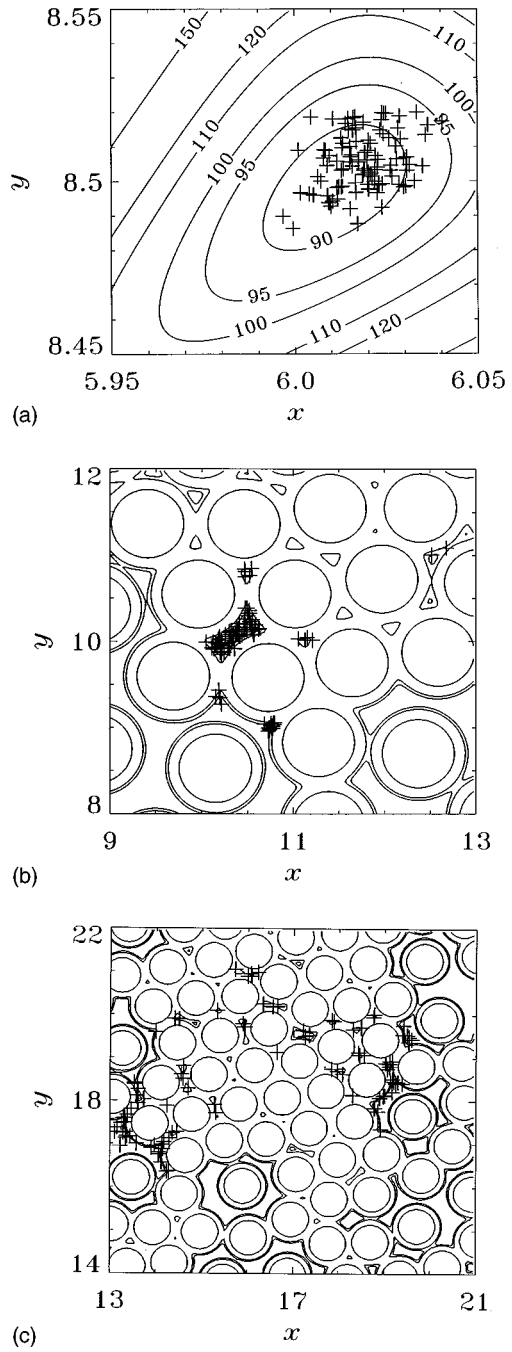

FIG. 1. Position of a single probe at a series of times (crosses) and local potential energy contours (lines), for (a) trapped probe at $k_BT=0.01$, (b) locally hopping probe at $k_BT=0.2$, and (c) diffusing probe at high temperature ($k_BT=1.0$).

shows a partly mobile probe able to reach four neighboring sites. Finally, at elevated temperatures (Fig. 1c shows $k_BT=1.0$), the probe is free to explore a substantial area.

At the lowest temperature, one finds simple trapping. The intermediate temperature shows hopping with long-time partial localization. The probe is able to sample several distinct sites, but (on the time scale studied here) is not mobile enough to travel large distances. At high temperature, one has hindered diffusion. The probe has preferred sites, but is able to move between many sites and covers distances much larger than a typical nearest-neighbor distance of a matrix particle.

How often does a probe migrate between sites? If one considers, e.g., the hopping probe of Fig. 1b, how often does that probe cross through the saddle points of $u(r)$? Records of coarse-grained probe trajectories reveal that jumps between local minima are frequent. Only rarely does the probe remain in the same locale for several steps. The simulation samples many crossings of local barriers, but probes remain within a local cluster of minima without being able to travel over the full cluster.

A more detailed description of probe motion through the glass was obtained by examining multiple trajectories and characterizing trajectories statistically. Figure 2 presents the probability distribution function $P(r,t)$ for displacement r during time interval t, at low, intermediate and high temperatures. The solid line corresponds to fixed t; with increasing t, particles become more and more likely to be found at large distances from their initial point.

Probes at low temperature ($k_BT=0.01$, Fig. 2a) show trapping, as also inferred above from other diagnostics. With increasing t, probes move out from the origin, gradually filling in the local maximum at $r\approx 0.3$; however, even at very long times the particles never travel appreciably farther than 0.4 units from their starting point. For $P(r,t)$, the peak near $r\approx 0$ and the local maximum near $r\approx 0.4$ appear to arise from characteristic forms for the potential energy surface. As seen in Figs. 1a and 1b, the potential energy minimum between three triangularly disposed matrix particles is a circle or oval, which contributes to $P(r,t)$ the large peak near $r\approx 0$. In contrast, if the minimum lies between four matrix particles [e.g., Fig. 1b, near (10.5, 10.0)], the potential energy minimum has a dumbbell outline. A probe may remain in a single dumbbell lobe (contributing to $P(r,t)$ for $r\approx 0$) or it may migrate between lobes (contributing to $P(r,t)$ for r comparable to a typical length of the dumbbell arm, which from Fig. 2a is inferred to be ≈ 0.3 units.)

Figure 2b shows localized hopping. At all but the smallest r, $P(r,t)$ increases monotonically with increasing t, corresponding to the increase in probable probe displacements at larger times. Careful examination of the figure reveals indications of barrier obstruction and tunneling at several distances, most prominently $r=$ 1.0, 2.3, 2.9, and 3.8. Qualitative signs of barrier obstruction and penetration are the same as in our previous paper. In each barrier location, at shorter times $P(r,t)$ declines very markedly with increasing r as the barrier location is passed. With increasing t, the decline in $P(r,t)$ with increasing r becomes substantially weaker, marking penetration of the barrier by the probe.

Figure 2c shows high-temperature ($k_BT=1.0$) hindered diffusive behavior. On this log-log plot, $P(r,t)$ has to first approximation a Gaussian form. In the region $0.6\leqslant r\leqslant 5$ and large t, small ripples can be seen superimposed atop the Gaussian. We interpret these ripples as arising from features in the two-point density of states $\rho^{(2)}(r)$; this explanation was previously tested successfully for probes diffusing through square lattices. Ripples are not apparent at shorter

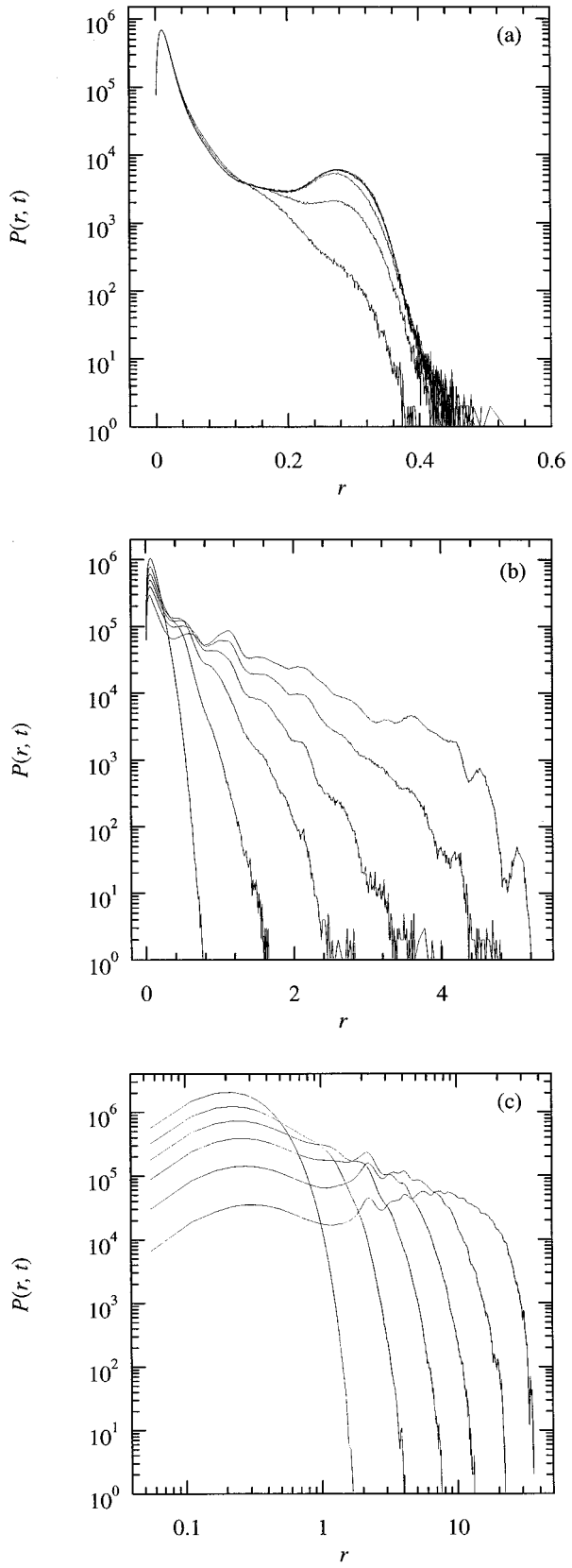

FIG. 2. Relative probability $P(r,t)$ of probe displacements r during a time interval t, plotted as a function of r; solid lines are at fixed $t=200\times1$, 200×10, 200×100, 200×10^3, 200×10^4, and 200×10^5. Temperatures k_BT are (a) 0.01, (b) 0.4, and (c) 1.0.

r because $\rho^{(2)}(r)$ lacks significant features at distances much less than the matrix particle size. P becomes relatively featureless at $r>5$ because in a glass the features of $\rho^{(2)}(r)$ wash out at large r, essentially for the same reasons that the radial distribution function $g(r)$ in a liquid becomes smooth at large r.

Scattering techniques are most typically sensitive to mean-square displacements against time, these being the second moment of $P(r,t)$. Figure 3 shows $\langle r^2(t)\rangle$ at low, intermediate and high temperatures. By comparison with our previous paper, we may readily identify these as showing trapping, hopping, and hindered diffusion, respectively, consistent with our above interpretations. One might have imagined that in a random system different probes would encounter very different patterns of obstacles, obscuring distinctions between motional regimes. However, even though the system lacks long range order, particle environments are sufficiently homogeneous that the different motional regimes are readily distinguished.

At $k_BT=0.01$ (Fig. 3a), $\langle r^2(t)\rangle$ increases at short times and then ceases to increase; rms probe displacements are ~0.05 at this time. From the study of probes in a regular lattice,[1] this behavior may be interpreted as showing a probe that rapidly explores the bounds of its trap and is then unable to move farther. At the intermediate $k_BT=0.2$ (Fig. 3b), $\langle r^2(t)\rangle$ increases rapidly over small distances; at longer displacements the increase of $\langle r^2(t)\rangle$ is less swift, corresponding (as in Ref.1) to a probe that first rapidly thermalizes its location over small distances via intratrap diffusion and then more gradually penetrates the barriers separating local minimum from local minimum.

The error bars, Fig. 3b, arise from the variation in $r^2(t)$ from particle to particle, due to the physical differences in the environments of different hopping particles; the statistical error in the computations is appreciably smaller.

Finally (Fig. 3c), at high temperature $\langle r^2(t)\rangle\sim t^1$ to good approximation at all t, a behavior characteristic of hindered diffusion. Observe that the ripples in $P(r,t)$ (Fig. 2c) have no appreciable impact on $\langle r^2(t)\rangle$. Conversely, there are interesting details of the diffusion process that are lost if one averages to the $\langle r^2(t)\rangle$ level. By calculating the more detailed full $P(r,t)$ rather than only calculating the second moment $\langle r^2(t)\rangle$, we are able to observe fine structure in the diffusion process that would not have been obvious from the second moment. It is noteworthy that simple t^1 behavior for $\langle r^2(t)\rangle$ sets in already at quite small $r(t)$, corresponding to rms displacements $\leqslant0.2$, contrary to any expectation that a probe needs to explore a substantial number of different sites (thereby covering distances $>1-2$ units) before hopping goes over to simple random-walk (central-limit-theorem) diffusive behavior.

Figures 3 and Eq. (5) allow calculation of an effective long-time diffusion coefficient D. Under trapping conditions, the resultant D is only a formal value. Figure 4 shows D/D_0 from our simulations. Here D_0 is the diffusion coefficient of a probe particle in the absence of the matrix. At $k_BT>0.8$ or so (open points), the probes perform restricted

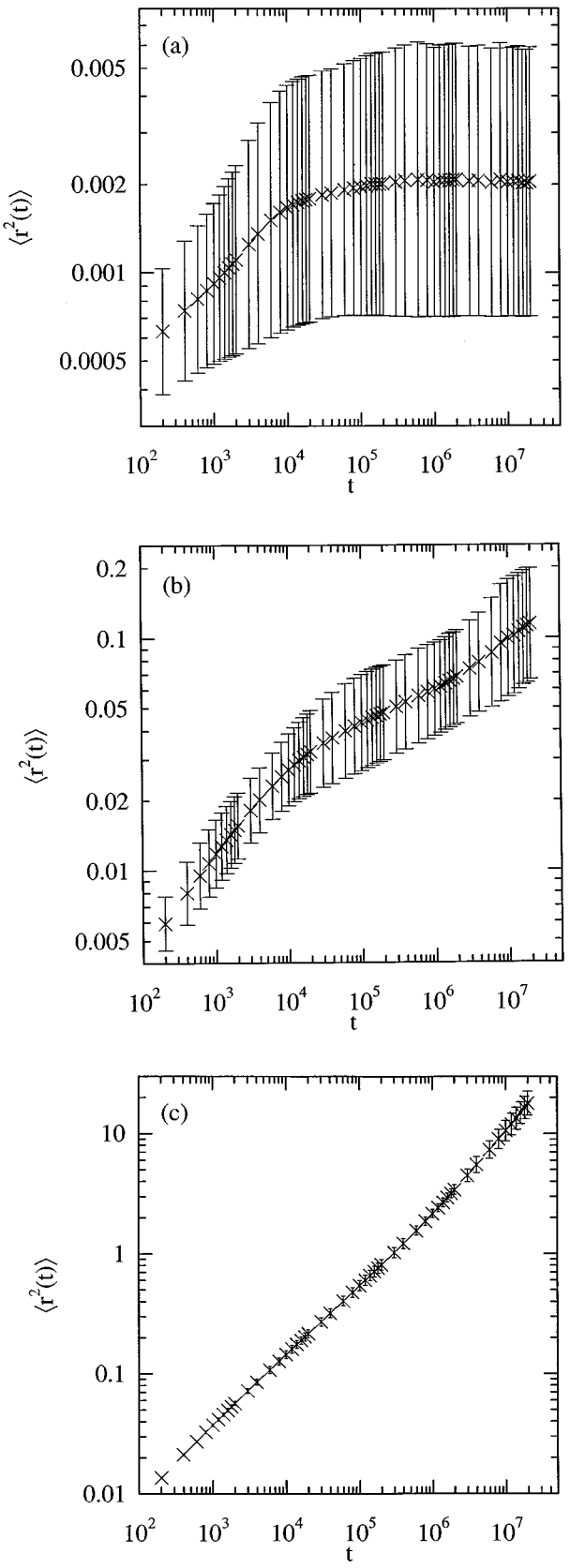

FIG. 3. Mean-square displacement $\langle r^2(t)\rangle$ as a function of time at under (a) trapping ($k_BT=0.01$), (b) localized hopping ($k_BT=0.2$), and (c) hindered-diffusive ($k_BT=1.0$) conditions.

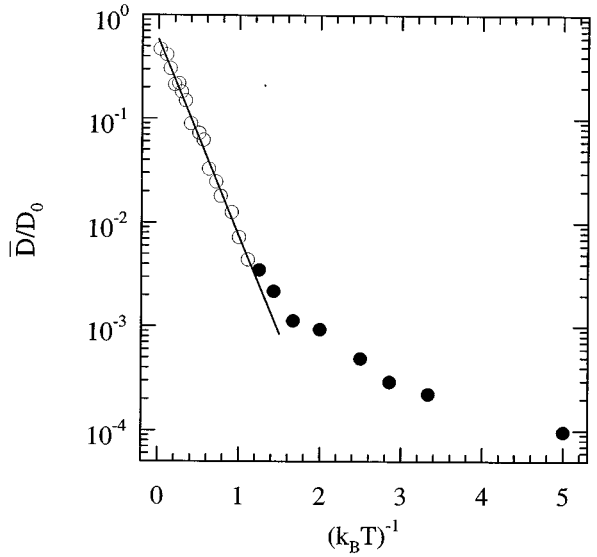

FIG. 4. Effective diffusion coefficient $\overline{D}$ (normalized to the diffusion coefficient D_0 of a probe in the absence of the matrix) as a function of inverse temperature $\beta=(k_BT)^{-1}$, showing Arrhenius behavior [solid line, Eq. (7)] at all temperatures at which the probe shows hindered diffusion. Filled dots show non-Arrhenius behavior in the lower-temperature hopping regime.

diffusion; $\overline{D}/D_0$ has simple Arrhenius behavior with activation energy $E_{\rm act}$:

$$\overline{D}/D_0 \sim \exp(-E_{\rm act}/k_BT). \tag{7}$$

At lower temperatures, probes move by hopping; Arrhenius behavior is not observed, $\overline{D}/D_0$ being larger than expected from Eq. (7).

Coherent scattering experiments, including light scattering spectroscopy using optical probes[2,3] and inelastic neutron scattering with isotropically labeled diffusants, measure the dynamic structure factor $S(\mathbf{k},t)$. If one has simple diffusive motion on all time and distance scales, then

$$S(\mathbf{k},t)=A\ \exp(-Dk^2t). \tag{8}$$

In this case, plots of $S(\mathbf{k},t)$ against t for various fixed k can be superposed (up to a scale factor A) by plotting $S(\mathbf{k},t)$ against k^2t.

Representative determinations of the dynamic structure factor appear in Figs. 5. At very low temperatures (Fig. 5a), probe particles are trapped; $S(\mathbf{k},t)$ only decays significantly at very large k, due to intratrap motion. With increasing temperature, probe hopping leads (Fig. 5b) to an increasing relaxation of $S(\mathbf{k},t)$, especially at larger k. With the onset of diffusive motion near $k_BT=1.0$, the relaxation of $S(\mathbf{k},t)$ down to $S(\mathbf{k},t)=0$ is readily observed (Fig. 5c). However, at $k_BT=1.0$, k^2t superposition is not observed. For the relaxations in Fig. 5c, D as defined by Eq. (8) depends substantially upon k. At very high temperature, (Fig. 5d), k^2t superposition is seen; D has become substantially independent of the length scale.

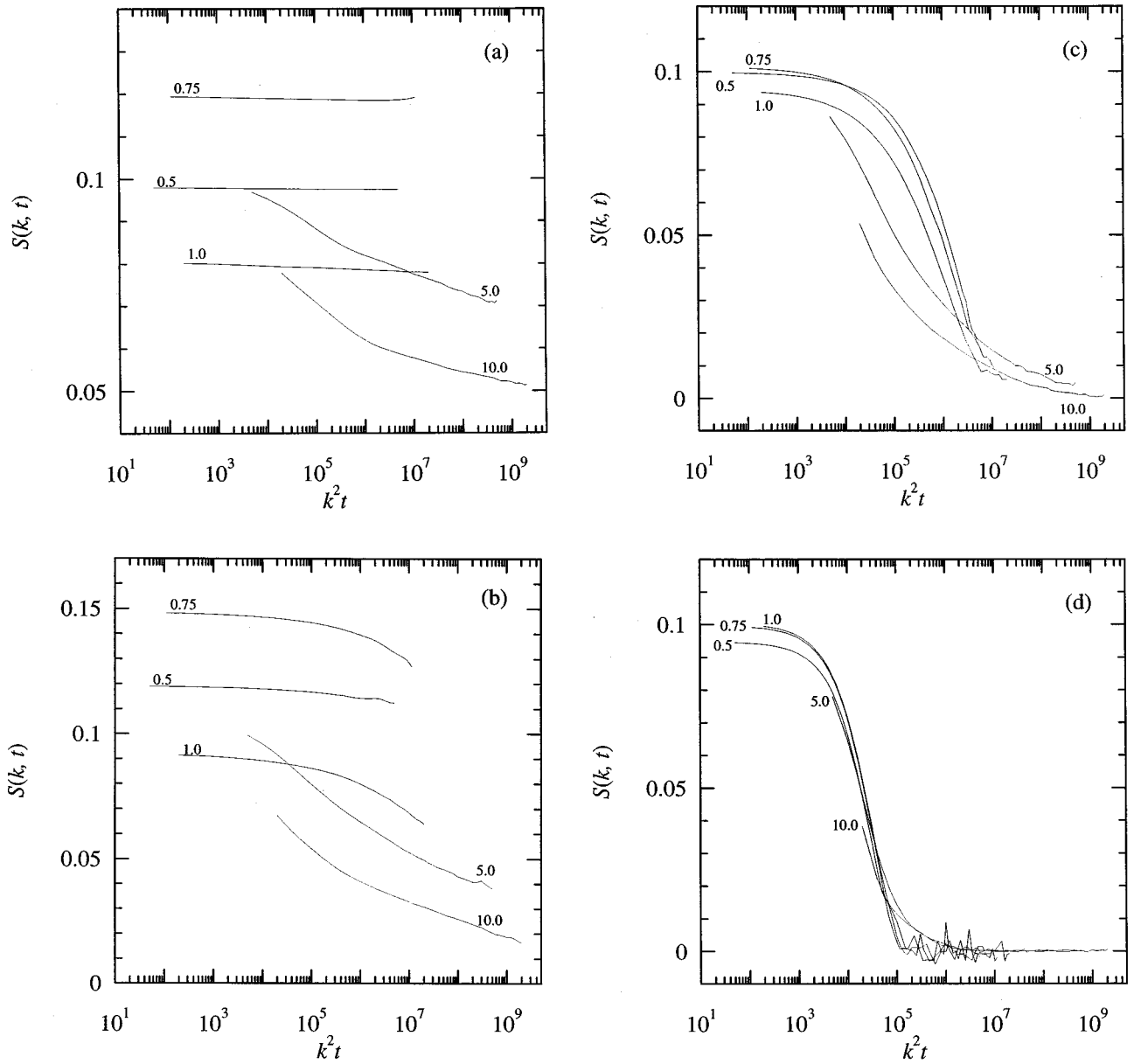

FIG. 5. $S(k,t)$ against reduced time k^2t with the same set of values of t for each fixed value of k, including (a) a trapping regime ($k_BT=0.15$), (b) a hopping regime with $k_BT=0.4$, and the diffusive regime $k_BT\geqslant 1.0$. D [Eq. (8)] is k-dependent at (c) $k_BT=1.0$, but is k-independent at (d) $k_BT=10.0$. Lines are functions of t at fixed k, values of k being 0.5, 0.75, 1.0, 5.0, and 10.0, the most extensive decay occurring at the largest k. $S(k,t)$ is obtained by averaging over multiple runs and over three directions for $\mathbf{k}$: parallel to $\hat{\mathbf{x}}$, to $\hat{\mathbf{y}}$, and to $\hat{\mathbf{x}}+\hat{\mathbf{y}}$.

IV. DISCUSSION

In this paper, we employed computer simulations and a wide variety of computational diagnostics, including trajectory plots, $P(r,t)$, $\langle r^2(t)\rangle$, and $S(\mathbf{k},t)$, to characterize the motion of a Brownian walker through a glassy array of force centers. As in our previous paper,[1] probe behavior fell into one of three regimes determined by temperature. Replacement of a regular lattice with an inhomogeneous glass did not obscure the distinction between trapping, hopping, and hindered-diffusive regimes. At the lowest temperatures, there was clear evidence of trapping behavior; probe particles were confined to individual local sites in the glass. At higher temperatures, we observed hopping motion, in which probe particles spend almost all of their time in localized sites, but are able on occasion to move from one site to the next. Particle motion in this regime is characterized by two distinct time scales, namely a fast time scale for intratrap motion and a slower time scale for motion between sites. The number of sites to which a given probe particle has access is temperature dependent; at larger T a wider range of sites is accessible, while time scales for intratrap and intertrap motion become less and less distinct. At sufficiently large T a hindered-diffusion regime, in which $\langle r^2(t)\rangle \sim t^1$, is entered. In the hindered-diffusion regime, D remains substantially less than its value in the absence of the matrix; D/D_0 is

temperature-dependent and follows an Arrhenius activation process.

$\langle r^2(t)\rangle$ is very nearly linear in t except at quite small times. From its definition, $\overline{D}$ refers to the long time limit of $\langle r^2(t)\rangle/4t$. Analytic computation of this limit would superficially appear to require a very-high-order time series expansion or the like. However, under hindered-diffusion conditions $\langle r^2(t)\rangle$ is extremely well behaved down to rather short times, so most of such a time series expansion is not needed. From the region in Fig. 3c in which linearity of $\langle r^2(t)\rangle$ against t sets in, a computation of mean-square probe motions adequate to treat particle displacements r of 0.1 or 0.2 units — these being displacements much smaller than the typical nearest-neighbor distance of lattice particles — must already be adequate to capture the features that determine $\overline{D}$. This surprising result indicates that a direct computation of $\overline{D}$ in a warm glass is more straightforward than might superficially have been expected.

We observe Arrhenius behavior for $\overline{D}/D_0$ in the diffusive regime, even at temperatures at which $\overline{D}$ is markedly k-dependent. The sensitivity to $\overline{D}$ to the range k^{-1} of particle displacements suggests the importance of different activation energies for motions through different distances. However, the activation energies for motion through different distances are sufficiently consistent that a single activation energy $E_{\rm act}$ remains adequate to describe the temperature dependence of $\overline{D}$.

ACKNOWLEDGMENTS

The partial support of this work by the National Science Foundation under Grant No. CHE91-15637 and by the Los Alamos National laboratory under Contract No. 9-XA3-4808L is gratefully acknowledged.

[1] L.-S. Luo, G. D. J. Phillies, L. Colonna-Romano, and H. Gould, Phys. Rev. E **51**, 43 (1995).
[2] Y. Guo, J. O'Donahue, K. H. Langley, and F. E. Karasz, Phys. Rev. A **46**, 3335 (1992).
[3] M. T. Bishop, K. H. Langley, and F. E. Karasz, Phys. Rev. Lett. **57**, 1741 (1986).
[4] F. Müller-Plathe, J. Chem. Phys. **94**, 3192 (1991).
[5] B. Y. Chen, H. Kim, S. D. Mahanti, T. J. Pinnavaia, and Z. X. Cai, J. Chem. Phys. **100**, 3872 (1994).
[6] I. Nishio, J. C. Reina, and R. Bansil, Phys. Rev. Lett. **59**, 684 (1987).
[7] I. H. Park, C. S. Johnson, Jr., and D. A. Gabriel, Macromolecules **23**, 1548 (1990).
[8] D. B. Sellen, in *Physical Optics of Dynamic Phenomena and Processes in Macromolecular Systems*, edited by B. Sedlacek (de Gruyter, Berlin, 1985), p. 177.
[9] K. Luby-Phelps, S. Mujumdar, R. B. Mujumdar, L. A. Ernst, W. Galbraith, and A. S. Waggoner, Biophys. J. **65**, 236 (1993).
[10] Yu. B. Mel'nichenko, V. V. Klepko, and V. V. Shilov, Europhys. Lett. **13**, 505 (1990).
[11] J. Newman, G. Gukelberger, K. L. Schick, and K. S. Zaner, Biopolymers **31**, 1265 (1991).
[12] Y. Suzuki and I. Nishio, Phys. Rev. B **45**, 4614 (1992).
[13] J. G. H. Joosten, E. T. F. Gelade, and P. N. Pusey, Phys. Rev. A **42**, 2161 (1990).
[14] L. Hou, F. Lanni, and K. Luby-Phelps, Biophys. J. **58**, 31 (1990).
[15] H. Gould and A. Melchuk (private communication).
[16] N. Metropolis, A. W. Rosenbluth, M. N. Rosenbluth, A. H. Teller, and E. Teller, J. Chem. Phys. **21**, 1087 (1953).
[17] W. H. Press, S. A. Teukolsky, W. T. Vetterling and B. P. Flannery, *Numerical Recipes in Fortran*, 2nd ed. (Cambridge University Press, New York, 1992).